TELKOMNIKA Telecommunication, Computing, Electronics and Control
Vol. 19, No. 2, April 2021, pp. 616~622
ISSN: 1693-6930, accredited First Grade by Kemenristekdikti, Decree No: 21/E/KPT/2018
DOI: 10.12928/TELKOMNIKA.v19i2.16706

The application of dual-layer remote phosphor geometry in achieving higher color quality of WLEDs

My Hanh Nguyen Thi[1], Phung Ton That[2], Hoang Van Ngoc[3]
[1]Faculty of Mechanical Engineering, Industrial University of Ho Chi Minh City, Viet Nam
[2]Faculty of Electronics Technology, Industrial University of Ho Chi Minh City, Vietnam
[3]Institute of Applied Technology, Thu Dau Mot University, Vietnam

Article Info

Article history:

Received May 16, 2020
Revised Aug 19, 2020
Accepted Sept 5, 2020

Keywords:

Color uniformity
Dual-layer remote phosphor geometry
Luminous flux
Mie-scattering theory
WLEDs

ABSTRACT

If remote phosphor structures are put into comparison with conformal phosphor or in-cup phosphor, their luminous flux are better, but the color quality is not as elevated. This leads to an obvious need of a practical solution to enhance color quality. Therefore, many studies were carried out to achieve this purpose, and so is ours. We proposed using two layers of phosphor in WLEDs to achieve better rendering ability and chromatic performance. The identical WLEDs with different color temperatures, 5600 K-8500 K, were used and reported in this paper. Our research consists of two parts, which are placing a layer of red phosphor $Sr_wF_xB_yO_z:Eu^{2+},Sm^{2+}$ on the yellow YAG:Ce^{3+} phosphor layer at first, and then specifying an appropriate $Sr_wF_xB_yO_z:Eu^{2+},Sm^{2+}$ concentration to reach the highest color performance. It is shown that with the contribution of $Sr_wF_xB_yO_z:Eu^{2+},Sm^{2+}$, the color rendering index (CRI) and color quality scale (CQS) are increased. This can be explained by the increased amount of red light components in the WLEDs when the concentration of $Sr_wF_xB_yO_z:Eu^{2+},Sm^{2+}$ was greater. However, excessive $Sr_wF_xB_yO_z:Eu^{2+},Sm^{2+}$ will cause the reduction in the flux, which has been proven by the application of Mie scattering and the Lambert-Beer law. Therefore, the conclusion will present an optimal amount of $Sr_wF_xB_yO_z:Eu^{2+},Sm^{2+}$ to obtain high color quality while minimizing the light loss.

Corresponding Author:

Hoang Van Ngoc
Institute of Applied Technology
Thu Dau Mot University, Vietnam
Email: ngochv@tdmu.edu.vn

1. INTRODUCTION

As the results of becoming the alternative to the conventional light source, the phosphor converted white light emitting diodes (pc-WLEDs), which is well known for high durability, lighting efficiency, and cost effectiveness, has provided various directions in the development of lighting solution [1-3]. Besides, there are some drawbacks related to transmission of light and the phosphor particles distribution still existing in this kind of light source, but it has become popular in many aspects of human life including backlighting and street lighting, lately [4, 5]. Moreover, the increasing demands of lighting market have created a need for a big leap regarding the lumen output as well as the chromatic performance of the white LEDs to multiply its applications [6, 7]. There have been many methods used to realistic this goal, and one of them was applying the combination of chromatic rays from components such as phosphor materials and LED chips [8-10]. Due to the significant impact of lighting device configuration and components organization on the luminous efficiency, especially the color rendering index [11, 12], the concept gained its recognition. In addition,

though many scientists recommended using common phosphor coating methods to produce LEDs such as conformal coating and dispensing coating [13, 14], these structures were not optimal to perform the best color quality. The reason is that the phosphor material is inferior in terms of light conversion due to the effect of constantly rising heat at the surface between the pc-WLEDs parts, which occurs because phosphor and LED chips do not have space to ventilate [15, 16].

Hence, color quality of white LEDs is only lifted if the phosphor is superior in conversing light and is not damaged by the heat from the LED chip. Therefore, a remote structure designed with a distance to separate the phosphor and the LED chip could become the ideal model, since it can reduce the mentioned effect, according to many previous researches [17, 18]. When the phosphor and the LED chip are set in an appropriate distance, the backscattering and circulation of the light inside the LED could be sufficiently minimized. Thus, the idea is recognized to be an efficient way of managing the heat of LED, by which the LEDs could be optimized in color quality and the luminous efficiency [19]. However, this lighting configuration is unable to adapt to all demands of illumination applications, as to the regular lighting, and therefore, it opened an opportunity for the next generation of LED to be fabricated. There have been some innovative remote phosphor structures suggested so far to advance the obtained luminous flux and reduce the back-scattering event occurred inside the LED. According to a study, placing reversed conial lens and arranging phosphor material in a circular form around the LED could adjust the direction to the LED surface of lights emitted from the inside chip. What is more, this structure can also dramatically reduce the light loss from the effects of internal reflection of the LED. It can be demonstrated that if an engraved remote model is set with an empty border while the surrounding is not covered with phosphor layers, it could lead to the high color uniformity and consistency by eliminating the distributed phosphor discrepancy at far angles. Furthermore, the remote phosphor also used the substrate as the sapphire pattern, which is more advantageous in getting greater color quality performance in far field pattern compared to older setup [20]. Hence, scientists proposed the remote phosphor with dual layer package in the effort of magnifying the performance of the light output of LEDs. However, there is an arduous obstacle we need to surmount: achieving better lighting performance for WLEDs with higher CCT [21, 22]. Although this issue is a pressing matter that can change the LEDs application in lighting industry, the aforementioned studies just focused on improving the color uniformity and luminescence of WLEDs by applying the remote phosphor structure with single chip WLEDs and low color temperatures [23].

In this research paper, we decided to use multi-layers WLEDs at different color temperatures from 5600 K to 8500 K and study their impacts on the optical properties. The innovative idea in this paper is that the red phosphor layer $Sr_wF_xB_yO_z:Eu^{2+},Sm^{2+}$ is applied to add needed phosphor particles for better color quality, and then the indexes of color rendering index (CRI) and color quality scale (CQS)could be also raised. Moreover, the noticeable effects of $Sr_wF_xB_yO_z:Eu^{2+},Sm^{2+}$ on the overall quality of resulted lights are also presented in this article. On top of that, the article has also provided useful results in which the values of quality indicators for rending ability and color output are positively affected by the $Sr_wF_xB_yO_z:Eu^{2+},Sm^{2+}$ phosphoric layer added in WLEDs. Besides, the paper has noted the importance in determining an appropriate level of $Sr_wF_xB_yO_z:Eu^{2+},Sm^{2+}$ concentration in order to avoid the deep decline in the flux of reddish phosphorus. In addition, it also mentioned two significant differences in terms of the yellow $YAG:Ce^{3+}$ phosphor covered by the red phosphor layer. One is increasing the constituent red light in the light emitted from WLEDs, which is one of the vital elements that contributing to the higher quality of color in WLEDs, and the other is the enhancement of scattered and transmitted light in WLEDs that are in the opposite trend to the concentration of $Sr_wF_xB_yO_z:Eu^{2+},Sm^{2+}$. Hence, it is extremely essential to decide a suitable value of $Sr_wF_xB_yO_z:Eu^{2+},Sm^{2+}$ concentrations to remain the stability in the photosensitivity of WLEDs.

2. RESEARCH METHOD

2.1. Material preparation

Table 1 showed the ingredients of $Sr_wF_xB_yO_z:Eu^{2+},Sm^{2+}$. From these figures, this compound can be calculated with the usage of the formula which was built by reckoning the molar percentage of each element. Besides, the detailed production process of $Sr_wF_xB_yO_z:Eu^{2+},Sm^{2+}$ can be described as following steps. Initially, Eu_2O_3 and Sm_2O_3 grains are dissolved in a dilute nitric acid solution while $Sr(NO_3)_2$ and H_3BO_3 are dissolved in warm water (90 ℃). Then, mixing these two solutions together and adding a solution containing acetone and ammonium hydroxide with the ratio of 1:1, and after that strongly stirring these mixtures. After a short time, there will be a fine white precipitate, and it will turn into a slurry. Next, heating this slurry at the temperature of 80 ℃ in two hours. After two hours, it will be cooled down to room temperature. Subsequently, this precipitate is filtered and dried in the air, blended with SrF_2 afterward, and then grinding the whole compound. The obtained compound is then burned in an open quartz crucible at 900 ℃ for about an hour. After being cooled down from 900 ℃, the compound is blended and ground into fine particles.

Later, these particles are fired at them same previous temperature for two hours, with the presence of a flow of H_2 in N_2 gas through the crucible. Finally, $Sr_wF_xB_yO_z:Eu^{2+},Sm^{2+}$ phosphor is produced after cooling and re-grounding the attained particles.

Table 1. Composition of red-emitting $Sr_wF_xB_yO_z:Eu^{2+},Sm^{2+}$ phosphor

Ingredient	Mole (%)	By weight (g)	Molar mass (g/mol)	Mole (mol)	Ions	Mole (mol)	Mole (%)
$Sr(NO_3)_2$	10.09	126.98	211.63	0.6	Sr^{2+}	0.6	0.0241
SrF_2	5.43	40.58	125.62	0.32	F^-	0.646	0.0259
H_3BO_3	84.12	309.2	61.83	5	B^{3+}	5	0.203
Eu_2O_3	0.25	5.28	351.93	0.015	O^{2-}	18.665	0.748
Sm_2O_3	0.11	2.09	348.72	0.006	Eu^{2+}	0.03	0.0012
		$Sr_wF_xB_yO_z:Eu^{2+},Sm^{2+}$			Sm^{2+}	0.012	0.00048

2.2. WLEDs modeling

To easily simulate the WLEDs with dual-layer phosphor structure, the LightTools 8.5.0 program and Mie-theory are the tools to conduct the experiments and verify the effect of $Sr_wF_xB_yO_z:Eu^{2+},Sm^{2+}$ phosphor on the performance of the WLEDs at the high correlated temperature, 5600-8500 K. Before structuring the in-cup phosphor configuration of WLEDs, the $Sr_wF_xB_yO_z:Eu^{2+},Sm^{2+}$ and YAG:Ce^{3+} phosphor are mixed together to form the phosphor layer of WLEDs. Specifically, this layer is comprised of red phosphor $Sr_wF_xB_yO_z:Eu^{2+},Sm^{2+}$ attached to the yellow phosphor YAG:Ce^{3+} with silicone gel.

As in Figure 1, the WLED configuration is formed by LED chips bounded to reflector cup, and phosphor layers held together with silicone. In specific, the chips are bonded with a reflector having a 2.07 mm depth, with a bottom length of 8 mm, and a 9.85 mm top length. In addition, the chip emits 1.16 W with a peak wavelength of 453 nm. The refractive index of $Sr_wF_xB_yO_z:Eu^{2+},Sm^{2+}$ and YAG:Ce^{3+} phosphor particle is fixed at 1.85 and 1.83, respectively. Moreover, to achieve the stability in average CCTs, there is an important note that the concentrations of YAG:Ce^{3+} and $Sr_wF_xB_yO_z:Eu^{2+},Sm^{2+}$ need to be adjusted to match each other.

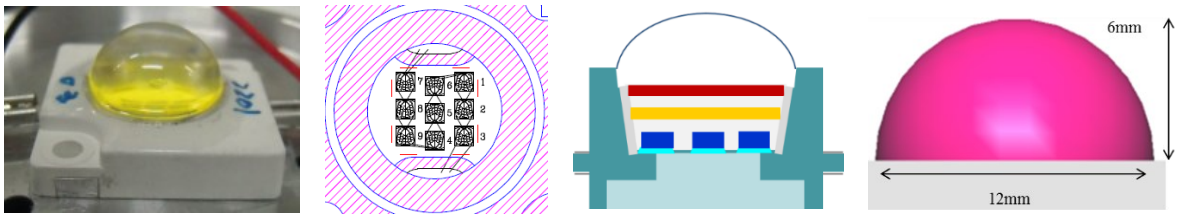

(a) (b) (c) (d)

Figure 1. Photograph of WLEDs structure: (a) actual WLEDs, (b) bonding diagram, (c) illustration of pc-WLEDs model, (d) simulation of WLEDs using LightTools commercial software

3. RESULTS AND ANALYSIS

There is a change that is opposite between the concentration of the $Sr_wF_xB_yO_z:Eu^{2+},Sm^{2+}$ red phosphor and the yellow phosphorus YAG:Ce^{3+}, as shown in Figure 2. The change can be understood as a mean to keep the color temperature at a stable value and ensure the obtained results of optical properties from WLEDs with different concentration of red phosphor is unaffected by the color temperature shifted unexpectedly. For that reason, determining and choosing an appropriate proportion of $Sr_wF_xB_yO_z:Eu^{2+},Sm^{2+}$ concentration are extremely crucial to the improvement in the color quality of WLEDs. It can be seen that with the increase in the $Sr_wF_xB_yO_z:Eu^{2+},Sm^{2+}$ concentration from 2% to 26% wt., the concentration of YAG:Ce^{3+} will be lowered to keep the color temperature at the primary value. Furthermore, the attained results are the same with different color temperatures of WLEDs, including 5600 K, 6600 K, 7000 K, 7700 K, or 8500 K.

The results presented from Figure 3 to Figure 7 illustrate the noticeable effects of the red phosphor $Sr_wF_xB_yO_z:Eu^{2+},Sm^{2+}$ concentration on the emission spectra of WLEDs. Based on the requirements from the manufacturers, the most suitable choice will be decided to achieve the highest efficiency. If they want to produce the high color quality WLEDs, it is able to reduce a small amount of luminescence to meet the demand. In fact, the nature of white light is the collection of the spectral regions as described in Figures 6-8.

In Figure 3, there are illustrations of the photosensitivity at 3 distinct CCT points from 5600-7700 K. Obviously, the wavelengths at which red light appears has increased, accompanying with the concentration of $Sr_wF_xB_yO_z:Eu^{2+},Sm^{2+}$. However, if the spectrum of the two remaining regions, 420-480 nm and 500-640 nm, are not in the rising trend, this result will become unimportant. In particular, the growth in the spectra at 420-480 nm boosts the amount of blue light in WLEDs. The fact that WLEDs from 5600 K and above created more emission points proves that the color temperature and spectra are compatible, and this results in higher color and luminosity, which means that the demands of manufacturers are completely fulfilled. Therefore, it is practical to apply the $Sr_wF_xB_yO_z:Eu^{2+},Sm^{2+}$ to produce WLEDs after considering how this application can solve the color performance issue in WLEDs. This study gave a solid statement that with $Sr_wF_xB_yO_z:Eu^{2+},Sm^{2+}$, manufacturers can successfully improve the color quality of WLEDs regardless of the low (5600 K) or higher (7700 K) color temperature.

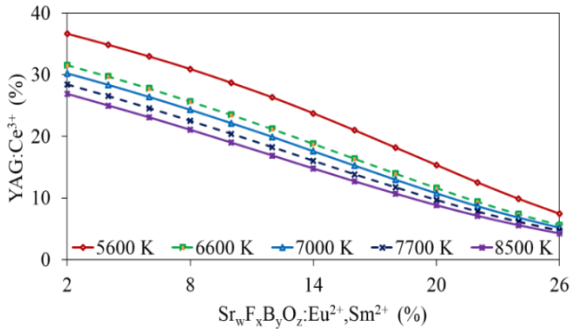

Figure 2. The change of phosphor concentration for keeping the average CCTs

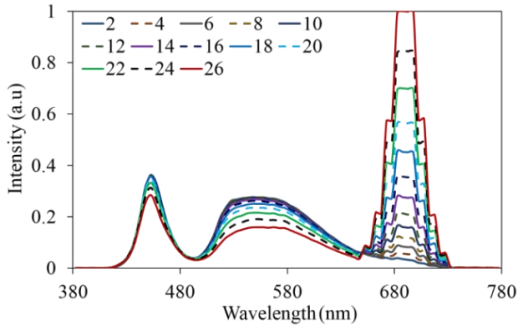

Figure 3. The emission spectra of 5600 K WLEDs as a function of $Sr_wF_xB_yO_z:Eu^{2+},Sm^{2+}$ concentration

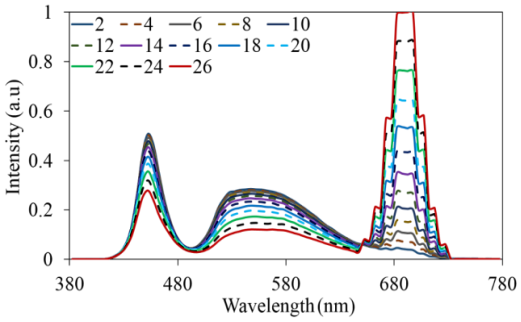

Figure 4. The emission spectra of 6600 K WLEDs as a function of $Sr_wF_xB_yO_z:Eu^{2+},Sm^{2+}$ concentration

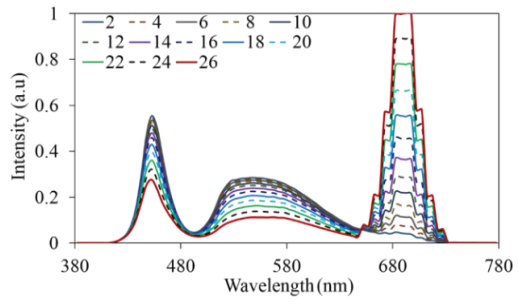

Figure 5. The emission spectra of 7000 K WLEDs as a function of $Sr_wF_xB_yO_z:Eu^{2+},Sm^{2+}$ concentration

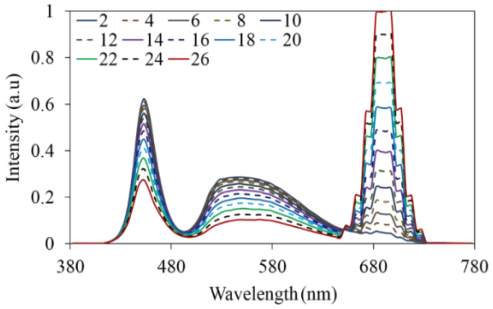

Figure 6. The emission spectra of 7700 K WLEDs as a function of $Sr_wF_xB_yO_z:Eu^{2+},Sm^{2+}$ concentration

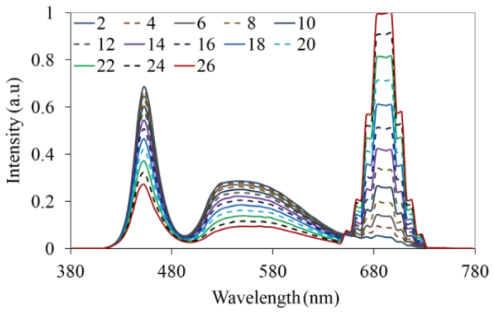

Figure 7. The emission spectra of 8500 K WLEDs as a function of $Sr_wF_xB_yO_z:Eu^{2+},Sm^{2+}$ concentration

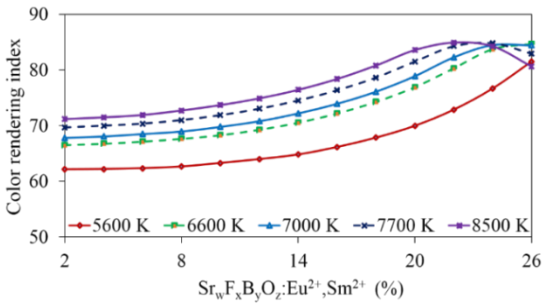

Figure 8. The color rendering index of WLEDs as a function of $Sr_wF_xB_yO_z:Eu^{2+},Sm^{2+}$ concentration

As shown in Figure 8, in all three different average CCTs, the $Sr_wF_xB_yO_z:Eu^{2+},Sm^{2+}$ phosphor concentration lifted the colorimetric index. This is because $Sr_wF_xB_yO_z:Eu^{2+},Sm^{2+}$ already transformed light from the chip to red light before it is absorbed. This is also the case for the light emitted from the yellow phosphor layer. Nevertheless, due to absorptive capacity discrepancy between blue and yellow light, more blue lights were absorbed than yellow ones. Hence, the result is obvious that the red light component in WLEDs increases when $Sr_wF_xB_yO_z:Eu^{2+},Sm^{2+}$ is added, heightening the CRI, which is considered as one of the most important parameters for modern WLED lamps. And when the color rendering index is high, it will push the price of each white light WLED. Nevertheless, with $Sr_wF_xB_yO_z:Eu^{2+},Sm^{2+}$, the WLEDs will be manufactured with lower cost. Consequently, $Sr_wF_xB_yO_z:Eu^{2+},Sm^{2+}$ has gained its popularity and widen its application. Nonetheless, we cannot evaluate the color quality of WLEDs just based on the color rendering index. Therefore, our study used a different quality indicator to evaluate the color of WLEDs, which is the CQS. CQS takes the color rendering index, the customer's personal choice, and the color coordinates to conclude the color performance of WLEDs. These factors have made CQS become an almost powerful general-quality color indicator.

In Figure 9 is the demonstration of the significantly lifted CQS values when the remote phosphor layer $Sr_wF_xB_yO_z:Eu^{2+},Sm^{2+}$ is in use. On top of that, when the concentration of $Sr_wF_xB_yO_z:Eu^{2+},Sm^{2+}$ is raised, the CQS also increased remarkably. The application of $Sr_wF_xB_yO_z:Eu^{2+},Sm^{2+}$ is confirmed to have a positive impact on the color quality of multi-layer WLEDs. Therefore, the result of this study is practical to the objective of improving color quality. However, $Sr_wF_xB_yO_z:Eu^{2+},Sm^{2+}$ also has drawback in output luminous flux. The part below is the mathematical equations to calculate the blue and yellow light in WLEDs with two-phosphor layers, from which an overall idea of how to improve the light output of WLEDs can be obtained. The following formulas demonstrate the blue light transmission and yellow light conversion for remote phosphor structure with one phosphor layer and *2h* phosphor thickness:

$$PB_1 = PB_0 \times e^{-2\alpha_{B1}h} \quad (1)$$

$$PY_1 = \frac{1}{2}\frac{\beta_1 \times PB_0}{\alpha_{B1}-\alpha_{Y1}}\left(e^{-2\alpha_{Y1}h} - e^{-2\alpha_{B1}h}\right) \quad (2)$$

The results of blue light transmission and yellow light conversion in dual-layer remote structure with the thickness *h* are expressed as follow:

$$PB_2 = PB_0 \times e^{-2\alpha_{B2}h} \quad (3)$$

$$PY_2 = \frac{1}{2}\frac{\beta_2 \times PB_0}{\alpha_{B2}-\alpha_{Y2}}\left(e^{-2\alpha_{Y2}h} - e^{-2\alpha_{B2}h}\right) \quad (4)$$

In which *h* is the thickness of each phosphor layer. In addition, single layer and double-layer remote phosphor package is demonstrated by the subscript "1" and "2". β is the conversion coefficient for blue light converting to yellow light. γ represents the reflection coefficient of the yellow light. The intensities of blue light (*PB*) and yellow light (*PY*) are the light intensity from blue LED, presented by PB_0. α_B; α_Y are used to describe the fractions of the energy loss of blue and yellow lights during their propagation in the phosphor layer, respectively. The significant enhancement that dual-layer remote phosphor WLEDs brings to the lumen output in comparison with the similar structure with one layer of phosphor is concluded from:

$$\frac{(PB_2+PY_2)-(PB_1+PY_1)}{PB_1+PY_1} > 0 \quad (5)$$

Besides, the Mie-theory [24, 25] is applied to analyze the scattering of $Sr_wF_xB_yO_z:Eu^{2+},Sm^{2+}$ phosphor grains. Moreover, based on the application of Mie-theory, an expression used to compute the scattering cross section C_{sca} for spherical particles can be formed as the following. The transmitted light power can be reckoned with the Lambert-Beer law:

$$I = I_0 \, exp(-\mu_{ext}L) \quad (6)$$

In this formula, I_0 indicates the incident light power, L is the phosphor layer thickness (mm), and μ_{ext} presents the extinction coefficient, which can be expressed as: $\mu_{ext} = N_r.C_{ext}$, where N_r is known as the number density distribution of particles (mm^{-3}). C_{ext} (mm^2) is the extinction cross-section of phosphor particles. (5) showed that dual-layer remote phosphor can result in the larger light output than structure with one layer. Nevertheless, the amount of $Sr_wF_xB_yO_z:Eu^{2+},Sm^{2+}$ phosphor also has a great impact on the light output of WLEDs with two phosphor layers. It can be easy to recognize through the Lambert-Beer law that, while being proportional to the concentration of $Sr_wF_xB_yO_z:Eu^{2+},Sm^{2+}$, the μ_{ext} attenuation coefficient is inversely proportional to the energy of light. Due to this result, under the condition that the density of phosphor layers is unchanged, the obtained flux could be weakened, even though $Sr_wF_xB_yO_z:Eu^{2+},Sm^{2+}$ concentrations rises. According to this, in Figure 10, the decrease in all five different CCTs is presented. When the concentration of $Sr_wF_xB_yO_z:Eu^{2+},Sm^{2+}$ reaches 26% wt., the flux obviously decreases. However, considering how $Sr_wF_xB_yO_z:Eu^{2+},Sm^{2+}$ benefit the color performance of WLEDs, it is worth to be taken into consideration. Moreover, comparing structures with and without the red phosphor layers, it is obvious that the WLEDs with red phosphors still emit much more lights. Therefore, a small loss in luminous flux would not affect much the overall performance. Furthermore, the appropriate could be determined depending on the purposes of manufacturers when mass producing this WLEDs.

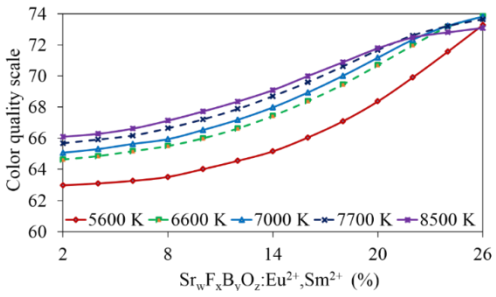

Figure 9. The color quality scale of WLEDs as a function of $Sr_wF_xB_yO_z:Eu^{2+},Sm^{2+}$ concentration

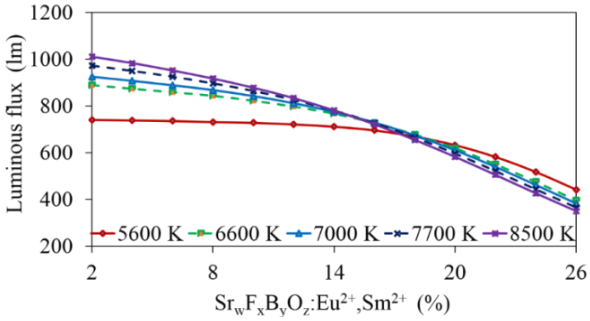

Figure 10. The luminous flux of WLEDs as a function of $Sr_wF_xB_yO_z:Eu^{2+},Sm^{2+}$ concentration

4. CONCLUSION

From the research paper, the $Sr_wF_xB_yO_z:Eu^{2+},Sm^{2+}$ effects on CRI and CQS of dual-layer phosphor structure are demonstrated. Through applying the Mie-theory of scattering and Lambert-Beer law, the choice of using $Sr_wF_xB_yO_z:Eu^{2+},Sm^{2+}$ in WLEDs for color quality enhancement is practical. This method also has the same response to WLEDs at all color temperatures, which is convenient for the different lighting applications. Therefore, this research has successfully reached the initial goal of improving white light quality, which is considered as a huge obstacle for remote-phosphor structures. However, it is noticed that a small drawback still exists in terms of the emission of the flux. Specifically, when the concentration of $Sr_wF_xB_yO_z:Eu^{2+},Sm^{2+}$ is redundant, the luminosity sharply declines. That is why it is extremely essential to decide an appropriate concentration, based on the objectives that manufacturers want to reach. Moreover, manufacturers can use this article for reference because it has provided a lot of practical information in producing a WLEDs' generation with better color quality.

REFERENCES

[1] J. Chen, *et al.*, "Microlens arrays with adjustable aspect ratio fabricated by electrowetting and their application to correlated color temperature tunable light-emitting diodes," *Opt. Express,* vol. 27, pp. A25-A38, 2019.

[2] T. Y. Orudzhev, *et al.*, "Increasing the extraction efficiency of a light-emitting diode using a pyramid-like phosphor layer," *J. Opt. Technol*, vol. 86, pp. 671-676, 2019.
[3] Z. Li, *et al.*, "Efficiency enhancement of quantum dot–phosphor hybrid white-light-emitting diodes using a centrifugation-based quasi-horizontal separation structure," *Opt. Express,* vol. 28, pp. 13279-13289, 2020.
[4] O. H. Kwon, *et al.*, "Simple prismatic patterning approach for nearly room-temperature processed planar remote phosphor layers for enhanced white luminescence efficiency," *Opt. Mater. Express,* vol. 8, pp. 3230-3237, 2018.
[5] A. Keller, *et al.*, "Diffuse reflectance spectroscopy of human liver tumor specimens-towards a tissue differentiating optical biopsy needle using light emitting diodes," *Biomed. Opt. Express,* vol. 9, pp. 1069-1081, 2018.
[6] M. Hu, *et al.*, "Broadband emission of double perovskite Cs2Na0.4Ag0.6In0.995Bi0.005Cl6:Mn2+ for single-phosphor white-light-emitting diodes," *Opt. Lett,* vol. 44, pp. 4757-4760, 2019.
[7] C. H. Lin, *et al.*, "Hybrid-type white LEDs based on inorganic halide perovskite QDs: candidates for wide color gamut display backlights," *Photon. Res,* vol. 7, pp. 579-585, 2019.
[8] N. Bamiedakis, *et al.*, "Ultra-Low Cost High-Density Two-Dimensional Visible-Light Optical Interconnects," *J. Lightwave Technol,* vol. 37, pp. 3305-3314, 2019.
[9] Z. Song, *et al.*, "Residual vibration control based on a global search method in a high-speed white light scanning interferometer," *Appl. Opt,* vol. 57, pp. 3415-3422, 2018.
[10] A. Krohn, *et al.*, "LCD-Based Optical Filtering Suitable for Non-Imaging Channel Decorrelation in VLC Applications," *J. Lightwave Technol*, vol. 37, pp. 5892-5898, 2019.
[11] S. R. Chung, *et al.*, "Full color display fabricated by CdSe bi-color quantum dots-based white light-emitting diodes," *Opt. Mater. Express,* vol. 8, pp. 2677-2686, 2018.
[12] A. Lihachev, *et al.*, "Differentiation of seborrheic keratosis from basal cell carcinoma, nevi and melanoma by RGB autofluorescence imaging," *Biomed. Opt. Express,* vol. 9, pp. 1852-1858, 2018.
[13] D. Lazidou, *et al.*, "Investigation of the Cross-Section Stratifications of Icons Using Micro-Raman and Micro-Fourier Transform Infrared, FT-IR. Spectroscopy," *Appl. Spectrosc*, vol. 72, pp. 1258-1271, 2018.
[14] Z. Zhang, *et al.*, "Tunable photoluminescence in $Ba_{1-x}Sr_xSi_3O_4N_2$: Eu^{2+}/ Ce^{3+}, Li^+ solid solution phosphors induced by linear structural evolution," *Opt. Mater. Express,* vol. 9, pp. 1922-1932, 2019.
[15] V. B. Yekta, *et al.*, "Limiting efficiency of indoor silicon photovoltaic devices," *Opt. Express,* vol. 26, pp. 28238-28248, 2018.
[16] J. H. Park, *et al.*, "High transmittance and deep RGB primary electrochromic color filter for high light out-coupling electro-optical devices," *Opt. Express,* vol. 27, pp. 25531-25543, 2019.
[17] Y. Sun, *et al.*, "Improving the Color Gamut of a Liquid-crystal Display by Using a Bandpass Filter," *Curr. Opt. Photon*, vol. 3, pp. 590-596, 2019.
[18] Y. Yang, *et al.*, "Low complexity OFDM VLC system enabled by spatial summing modulation," *Opt. Express,* vol. 27, pp. 30788-30795, 2019.
[19] Y. Li, *et al.*, "395 nm GaN-based near-ultraviolet light-emitting diodes on Si substrates with a high wall-plug efficiency of 52.0%@350 mA," *Opt. Express,* vol. 27, pp. 7447-7457, 2019.
[20] Y. Fei, *et al.*, "Luminescence properties of KBaYSi2O7:Ce/Eu-Tb phosphors for multifunctional applications," *Appl. Opt,* vol. 58, pp. 4740-4745, 2019.
[21] A. Ahmad, *et al.*, "Characterization of color cross-talk of CCD detectors and its influence in multispectral quantitative phase imaging," *Opt. Express,* vol. 27, pp. 4572-4589, 2019.
[22] J. Lui, *et al.*, "Preliminary design and characterization of a low-cost and low-power visible light positioning system," *Appl. Opt,* vol. 58, pp. 7181-7188, 2019.
[23] F. Jiang, *et al.*, "Efficient InGaN-based yellow-light-emitting diodes," *Photon. Res*, vol. 7, pp. 144-148, 2019.
[24] J. Cheng, *et al.*, "Luminescence and energy transfer properties of color-tunable Sr_4La , $PO_{4.3}O$: Ce^{3+}, Tb^{3+}, Mn^{2+} phosphors for WLEDs," *Opt. Mater. Express,* vol. 8, pp. 1850-1862, 2018.
[25] P. Zhu, *et al.*, "Design rules for white light emitters with high light extraction efficiency," *Opt. Express,* vol. 27, pp. A1297-A1307, 2019.